Paz-Cedeno, FR.; Carceller-Carceller, JM.; Iborra Chornet, S.; Donato, RK.; Godoy, AP.; De Paula, AV.; Monti, R.... (2021). Magnetic graphene oxide as a platform for the immobilization of cellulases and xylanases: Ultrastructural characterization and assessment of lignocellulosic biomass hydrolysis. Renewable Energy. 164:491-501. https://doi.org/10.1016/j.renene.2020.09.059

Magnetic graphene oxide as a platform for the immobilization of cellulases and xylanases: ultrastructural characterization and assessment of lignocellulosic biomass hydrolysis

Fernando Roberto Paz-Cedeno,[*a] Jose Miguel Carceller,[b] Sara Iborra,[b] Ricardo Keitel Donato,[c] Anna Paula Godoy,[d] Ariela Veloso de Paula,[a] Rubens Monti,[a] Avelino Corma[*b] and Fernando Masarin[a]

[a]São Paulo State University (UNESP), School of Pharmaceutical Science (FCF), Department of Bioprocess Engineering and Biotechnology. Araraquara-SP, Brazil. 14800-903

[b]Universitat Politècnica de València (UPV), Institute of Chemical Technology (ITQ), Valencia, Spain. 46022

[c]Institute of Macromolecular Chemistry, Czech Academy of Sciences, Prague, Czech Republic.162 06

[d]Graphene and Nanomaterials Research Center, Mackenzie Presbyterian University, São Paulo, Brazil. 01302-907

(*) Corresponding author

Email addresses:

FRPC: fernando.paz@unesp.br
JMC: jocarca8@upvnet.upv.es
SI: siborra@itq.upv.es
RKD: donato@imc.cas.cz
APG: apaulasgodoy@gmail.com
AVP: ariela.veloso@unesp.br
RM: rubens.monti@unesp.br
AC: acorma@itq.upv.es
FM: fernando.masarin@unesp.br

ABSTRACT

For producing second-generation ethanol (cellulosic ethanol) and other value-added bioproducts, magnetic graphene oxide (GO-MNP) was synthesized in this work and used as the immobilization support for an industrial cellulase and xylanase-containing preparation. GO-MNP characterization by TEM, SEM and ATR-FTIR spectroscopy showed that the magnetic nanoparticles are homogeneously distributed onto the GO sheets surface. The enzymatic preparation was immobilized by means of carbodiimide cross-linking chemistry using 1-ethyl-3-(3-dimethylaminopropyl) carbodiimide and *N*-hydroxysuccinimide (NHS). The supported final biocatalyst (GO-MNP-Enz) showed high activity for the hydrolysis of pretreated sugarcane bagasse (PSB) and presented relative endoglucanase, xylanase, β-glucosidase, and β-xylosidase activities of 70%, 66%, 88%, and 70%, respectively, after 10 cycles of hydrolysis of their respective substrates. The biocatalyst also maintained approximately 50% and 80% of its efficiency for cellulose and xylan hydrolysis, respectively, being the TOF ($g.g^{-1}.h^{-1}$) the highest observed when compared with previous results observed in literature. These findings suggest that GO-MNP-Enz may be a prospective candidate for industrial applications such as second-generation ethanol production.

Keywords: Enzyme immobilization, graphene oxide, magnetic nanoparticles, biocatalyst, sugarcane bagasse hydrolysis, monomeric fermentable sugars

INTRODUCTION

Brazil is the largest exporter and second-largest producer (after the USA) of ethanol in the world, having produced approximately 33 billion liters in 2019 [1,2]. First-generation ethanol is mainly obtained from sugarcane and corn, while second-generation ethanol is derived from lignocellulosic biomass found in plants. An important step in the production of second-generation ethanol is the biocatalytic process that uses cellulases and xylanases to hydrolyze lignocellulosic material into fermentable sugars.

Biocatalytic processes have been applied in several sectors of the biotechnology due to their high specificity and conservation of the environment. However, the use of enzymes in industrial applications may be limited depending on their cost, which is a bottleneck in the production process of second-generation ethanol. In addition, maintaining the structural stability of some enzymes during any biochemical reaction is a major challenge [3].

The immobilization of enzymes onto solid supports offers many advantages, including reuse of the enzyme, relatively easy separation of the product, and increased enzyme stability [4]. Typically, the supports used for enzyme immobilization are agarose, sepharose, silica gel, chitosan, silica-based carriers, polysaccharide derivatives, synthetic polymers, and zeolites [5–12]. Since the support's surface area is a major characteristic for effective enzyme immobilization, two-dimensional (2D) materials, which include graphene and graphene oxide (GO), are exceptionally interesting for this application [13]. GO is an especially versatile chemical platform due to the vast availability of functional groups on its immense surface area (as high as 736.6 $m^2.g^{-1}$ in aqueous solutions) [14], making it an excellent support material for immobilizing enzymes [15,16]. The magnetization of the supports prior to use has shown great potential for recyclable applications [17–19]. A key advantage of using magnetic support for enzyme immobilization is the possibility to recover the supported biocatalyst using an external magnet, which is more viable in comparison to other recovery methods, such as filtration and centrifugation [20]. Recently several published works have developed such types of magnetic composite supports for the immobilization of enzymes [21,22].

Cellulases and xylanases immobilization in solid supports had been studied in the past [23–28]. However, in spite of various immobilization techniques and supports reported in the literature, there is still a demand for more efficient methods and easier recycling of the biocatalyst. This paper aims to add to the literature on the hydrolysis of lignocellulosic biomass using immobilized enzymes.

Considering the aforementioned, in this study GO-magnetic nanoparticles (GO-MNP) was synthesized and used as the immobilization support for a commercial enzymatic preparation containing cellulase and xylanase activities. Considering the nature of the support GO rich in acids groups, the covalent immobilization was carried out by activating the acid groups on the GO-MNP surface using 1-ethyl-3-(3-dimethylaminopropyl) carbodiimide (EDC) and then reacting with *N*-hydroxysuccinimide (NHS), providing a reactive site for enzyme immobilization (see Figure 1) [21,29–31]. The support and biocatalyst were ultrastructurally characterized and assessed for reuse using both specific substrates and an actual lignocellulosic material (sugarcane bagasse).

EXPERIMENTAL METHODS

Synthesis of GO and GO-MNP

GO was prepared using a modified version of Hummers' method [32]. Accordingly, graphite powder (99.99%; < 150 µm; Sigma-Aldrich, St. Louis, MO, USA) was mixed with H_2SO_4 (95-97% v/v) and oxidized to graphite oxide using $KMnO_4$. An aqueous suspension of graphite oxide (1 mg.mL^{-1}) was exposed to sonication for 2 h to exfoliate into GO. GO-MNP was obtained by co-precipitation of iron salts [17]. Briefly,

$FeCl_3 \cdot 6H_2O$ and $FeCl_2 \cdot 4H_2O$ (molar ratio 2:1) were added to an acetic acid solution (3% v/v) under vigorous stirring, and a GO dispersion (5 $mg.mL^{-1}$) was added. Then, the temperature was raised to 80 °C, and pH was increased by adding ammonia (25% v/v). Finally, the reaction was stopped, and the solid was collected using an external magnet and washed with ultrapure water and methanol. The solid was dried and stored. Before use, the material was exposed to sonication for 2 h in an aqueous suspension to exfoliate into GO-MNP.

Immobilization of cellulases and xylanases from enzymatic preparation on GO-MNP

The GO-MNP was functionalized to allow for the covalent immobilization of enzymes. For this purpose, 20 mL of a GO-MNP dispersion (0.5 $mg.mL^{-1}$) in acetate buffer (0.05 M; pH 4.8) was sonicated for 2 h. Next, 20 mg of NHS and 24 mg of EDC were added, and the mixture was stirred for 3 h. The solid was collected using an external magnet and washed with the same buffer. Subsequently, the solid was resuspended in acetate buffer (pH 4.8), and a volume (3-120 µL) of enzyme preparation Cellic CTec 2 (Novozymes, Denmark) was added. The suspension was placed on a rolling agitator at 120 rpm for 12 h. Finally, the biocatalyst was collected using an external magnet, washed with acetate buffer (pH 4.8), and resuspended in the same buffer. This biocatalyst was denoted as GO-MNP-Enz.

Ultrastructural characterization

Scanning electron microscopy (SEM) images and energy-dispersive X-ray (EDX) spectra were taken using an AURIGA Focused Ion Beam Scanning Electron Microscope (Zeiss, Germany). For this purpose, the samples were thoroughly dried in a vacuum oven and placed on a conductive carbon adhesive tape. Transmission electron microscopy (TEM) images and EDX spectra were recorded on a JEM-2100F Transmission Electron Microscope (JEOL, Japan). The samples were dispersed (≈ 0.04 $mg.mL^{-1}$) in ultrapure water (18.2 MΩ cm) and transferred to nickel square mesh grids. EDX spectra analysis provided elemental identification and quantitative compositional information. Atomic force microscopy (AFM) images were recorded on a MultiMode 8 Atomic Force Microscope under tapping mode (Bruker, USA). The samples were prepared by dispersing GO-MNP-Enz in aqueous solution (≈ 0.04 $mg.mL^{-1}$), placing it over a mica surface, and allowing the solvent to evaporate. Raman spectroscopy measurements were recorded using an alpha 300 R confocal microscope spectrometer (WITec, Germany) using 50× objective lens and grading of 600 $g.mm^{-1}$. A 532 nm excitation laser was employed to characterize the GO. A silicon oxide substrate was used to calibrate the spectrometer. The specific surface area of the GO and GO-MNP were calculated by the Brunauer-Emmet-Teller method (BET) by means of nitrogen adsorption at -196°C using an ASAP 2420 (V2.09 J). Lastly, the dried samples were subjected to infrared analysis using attenuated total reflection with a Fourier transform infrared (ATR-FTIR) spectrometer (Platinum-ATR Alpha; Bruker) with a single reflection diamond module.

Enzymatic activity assays

Total cellulase activity was determined according the methodology described by Ghose[33] with some modifications. Briefly, a filter paper strip (1.0 × 6.0 cm; ≈ 50 mg; Whatman No. 1) was used as the substrate in 1.2 mL of acetate buffer (pH 4.8) and 0.3 mL of enzymatic preparation Enz or biocatalyst suspension for free- or immobilized-enzymes, respectively. Endocellulase activity was measured using the methodology described by Tanaka *et al.* [34]. Accordingly, 0.9 mL of 0.44% (w/v) sodium carboxymethylcellulose (CMC) (≥ 95%; Carbosynth, USA) solution was placed in a tube, and 0.1 mL of Enz or immobilized biocatalyst suspension was added. For xylanase activity determination, we followed the methodology described by Bailey *et al* [35]. Thus, 0.9 mL of 1% (w/v) xylan (≥ 90%; Sigma-Aldrich) solution was added to 0.1 mL of Enz or immobilized biocatalyst suspension. The reactions of total cellulase, endoglucanases and xylanase activities were stopped by adding a volume of 3,5-Dinitrosalicylic acid (DNS), boiled for 5 min, and cooled before their respective absorbances were read at 540 nm.

β-glucosidase and β-xylosidase activities were measured according to Tan *et al* [36]. Following this method, 0.8 mL of 0.1% (w/v) 4-Nitrophenyl β-D-glucopyranoside (≥ 98%; Sigma-Aldrich) or 4-Nitrophenyl β-D-xylopyranoside (≥ 98%; Sigma-Aldrich) solution was added to 0.2 mL of Enz or immobilized biocatalyst suspension, respectively. The reactions were stopped by adding 2 mL of $NaHCO_3$, and the respective absorbances were read at 410 nm.

Yield, efficiency, and recovery activities of the enzyme immobilization were determined according to Equations 1, 2, and 3, respectively [37].

$$Yield = \left(\frac{A_i - A_f}{A_i}\right) * 100\% \quad \text{(Equation 1)}$$

$$Efficiency = \left(\frac{A_b}{A_i - A_f}\right) * 100\% \quad \text{(Equation 2)}$$

$$Activity\ recovery = \left(\frac{A_b}{A_i}\right) * 100\% \quad \text{(Equation 3)}$$

where A_i: total activity on the supernatant before immobilization, A_f: total activity on the supernatant after immobilization, and A_b: total activity on the biocatalyst.

Reuse of immobilized enzymes

To determine the reusability of the immobilized enzymes, GO-MNP-Enz was subjected to catalytic activity assays according to the previously described methods (endoglucanase, xylanase, β-glucosidase, and β-xylosidase). After the activity assay, GO-MNP-Enz was collected with an external magnet, washed with acetate buffer, and then reused into a new activity assay. The turnover frequency (TOF), defined as g of product obtained per g of biocatalyst per h, was calculated for the enzymatic hydrolysis of the respective substrates.

Hydrolysis of pretreated sugarcane bagasse (PSB)

One hundred grams of original sugarcane bagasse (dry basis) and 1 L of a Na_2SO_3 2% (w/v) and NaOH 1% (w/v) solution were added into a 1.5 L reactor (AU/E-20; Regmed, Brazil), culminating in a 1:10 ratio between the bagasse mass (dry basis) and solution volume. The reactor was closed and set to 140 °C and 4 rpm of horizontal rotation for 30 min [38]. Subsequently, the PSB was washed several times with distilled water and dried at 40 °C for 48 h. For the PSB hydrolysis using GO-MNP-Enz, 10 mg of

PSB (dry basis) was added to 10 mL of acetate buffer (pH 4.8) in an Erlenmeyer flask. Then, 150 mg of GO-MNP-Enz (44 FPU.g^{-1}) was added, and the reaction was carried out in a thermal bath at 30 °C and 120 rpm of shaking. After 24 h of hydrolysis, the GO-MNP-Enz was recovered using an external magnet, washed several times with acetate buffer (pH 4.8), and reused in a new hydrolysis cycle. The supernatant was recovered and used to determine sugars. This analysis was performed by high performance liquid chromatography (HPLC; C-R7A; Shimadzu, Japan) equipped with a HPX87H column (Bio-Rad, USA) at 60 °C in the isocratic mode using 0.005 M H_2SO_4 as a mobile phase at a flow rate of 0.6 mL.min^{-1} and detected using a RID-20A Refractive Index Detector (Shimadzu) at 60 °C [39–41]. The cellulose and xylan conversions were determined by Equations 4 and 5, respectively.

$$Cellulose\ conversion\ (\%) = \left(\frac{M_g * 0.9}{F_C * M_B}\right) * 100\% \quad \text{(Equation 4)}$$

$$Xylan\ conversion\ (\%) = \left(\frac{M_x * 0.88}{F_X * M_B}\right) * 100\% \quad \text{(Equation 5)}$$

where M_g: mass of glucose (mg) after a hydrolysis cycle, 0.9: conversion factor of glucose to cellulose, F_C: cellulose fraction in the dry PSB (g.g^{-1}), M_B: mass of PSB at the start of the reaction (mg), M_X: xylose concentration (mg) after a hydrolysis cycle, 0.88: conversion factor of xylose to xylan, and F_X: xylan fraction in the dry PSB (g.g^{-1}).

RESULTS AND DISCUSSION

Synthesis and characterization of the biocatalyst (GO-MNP-Enz)

Firstly, GO was obtained from graphite powder, and magnetic nanoparticles were attached onto the surface by coprecipitation of Fe^{2+} and Fe^{3+}. Then, the support was functionalized to allow for enzyme immobilization. Figure 1a shows a general scheme of

the synthesis and functionalization of the support, and Figure 1 and c displays the magnetic behavior of GO-MNP-Enz.

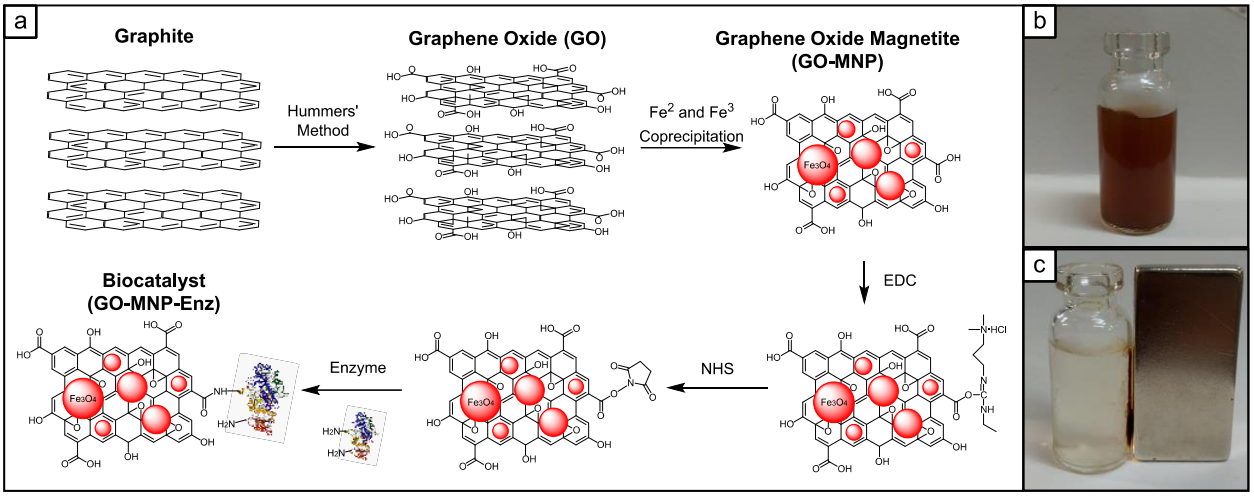

Figure 1. (a) Scheme of graphene oxide magnetite (GO-MNP) synthesis, functionalization and enzyme immobilization. Biocatalyst (GO-MNP-Enz) before **(b)** and after **(c)** apply an external magnetic field.

The ATR-FTIR spectra of GO, GO-MNP, GO-MNP-Enz, and Enz are depicted in Figure 2. The band at 570 cm^{-1}, present in the GO-MNP and GO-MNP-Enz systems, has been attributed to the elongation of the Fe-O bond within the crystalline network of Fe_3O_4 [42–45]. Thus, the presence of this band in GO-MNP indicates its successful magnetization, hence the absence of this band in GO. The band at 1040 cm^{-1} in the GO-MNP-Enz and Enz spectra has been attributed to C-N bond vibration [46,47]. The band observed at approximately 1540 cm^{-1} has been associated with C-N stretching and N-H bending vibrations in the -CONH groups [47]. The absence of these bands (1040 and 1540 cm^{-1}) in the GO-MNP spectrum showed that the enzymes were successfully immobilized on the support. The bands at 1640 and 3280 cm^{-1} correspond to deformation and stretching vibrations, respectively, of the O-H type connection in strongly intercalated water [48]. Additionally, Raman spectra (Figure S1) were collected

to evaluate the produced GO. According to the average multiple curve of GO (Figure S1), the D, G, and 2D bands are positioned at 1345, 1591 and 2669 cm^{-1}, respectively. The prominent D band with an intensity comparable to the G band indicates an important structural disorder because of the presence of oxygenated groups from GO. The G band is wider than the related to graphite powder, reinforcing structural changes with the insertion of defects [49]. The weak and broad 2D band is another indication of disorder. Near 2950 cm^{-1}, a defect-activated band denoted as D+G was also visible [50]. The I_D/I_G ratio was found to be 1.22, a value that represents a high quantity of defects in the formed GO.

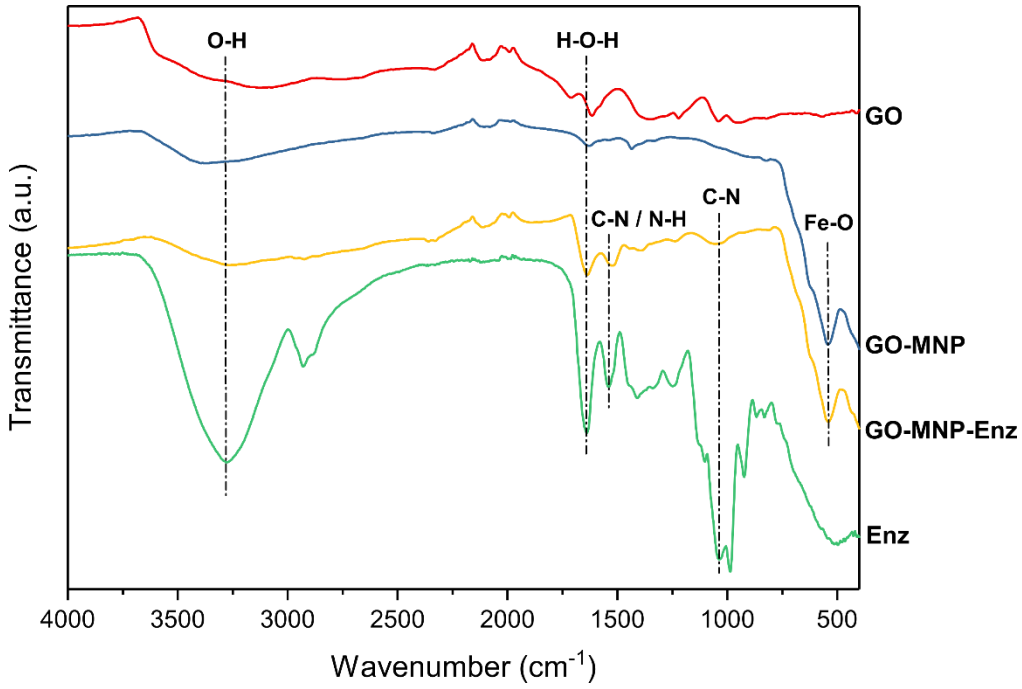

Figure 2. Total attenuated reflection in the infrared with Fourier transform (ATR-FTIR) spectrum of graphene oxide (GO), graphene oxide with magnetic nanoparticles (GO-MNP), biocatalyst (GO-MNP-Enz) and commercial enzymatic cocktail (Enz).

The SEM images show the morphology of the material before ultrasonic exfoliation, where the surface morphological aspect of the graphite oxide has the shape of overlapping sheets (Figure 3a) as noted by previous reports in the literature [48,51]. It

is possible to see the magnetic nanoparticles on the surface of graphite oxide generating graphite oxide-magnetite (Figure 3b). The elemental EDX analysis demonstrates that the graphite oxide-magnetite is formed by atoms of C, Fe, and O (Figure 3d) while the graphite oxide does not contain Fe in its structure (Figures S2a and b), confirming that the iron nanoparticles have adhered to the GO-MNP surface.

Graphite oxide and graphite oxide-magnetite were further exfoliated to form GO and GO-MNP, respectively, and were characterized by TEM-EDX analysis. TEM images of GO (Figure 3c) showed that monolayer and few-layer GO was obtained after exfoliation, also confirming that the magnetic nanoparticles remained onto the GO sheets' surface and were homogeneously distributed (Figure 3d). The EDX spectra showed that GO (Figure S2c) is composed exclusively of C and O while GO-MNP (Figure S2d) presents C, Fe, and O in its composition, paralleling the SEM-EDX results (Figures S2a and S2b). The presence of nickel in the EDX spectrum is attributed to the interference of the grid that is used as a support for the sample. Moreover, by analyzing the AFM height profile of GO-MNP-Enz (Figure 3f), it is possible to verify that the enzymes are immobilized on a single layer of GO since the height of the support is approximately 1 nm. BET analysis was performed to investigate the specific surface area of the materials. The surface area of the graphite oxide was 12 $m^2.g^{-1}$. This low value is probably due to the fact that nitrogen molecules cannot penetrate the interlaminar space of the dry graphite oxide. After the magnetization, the surface area was larger (103 $m^2.g^{-1}$), probably because the magnetite particles in the structure allowed a separation between layers of graphite oxide and the nitrogen could be absorbed. The both results were consistent with the literature [48,52–55]. The

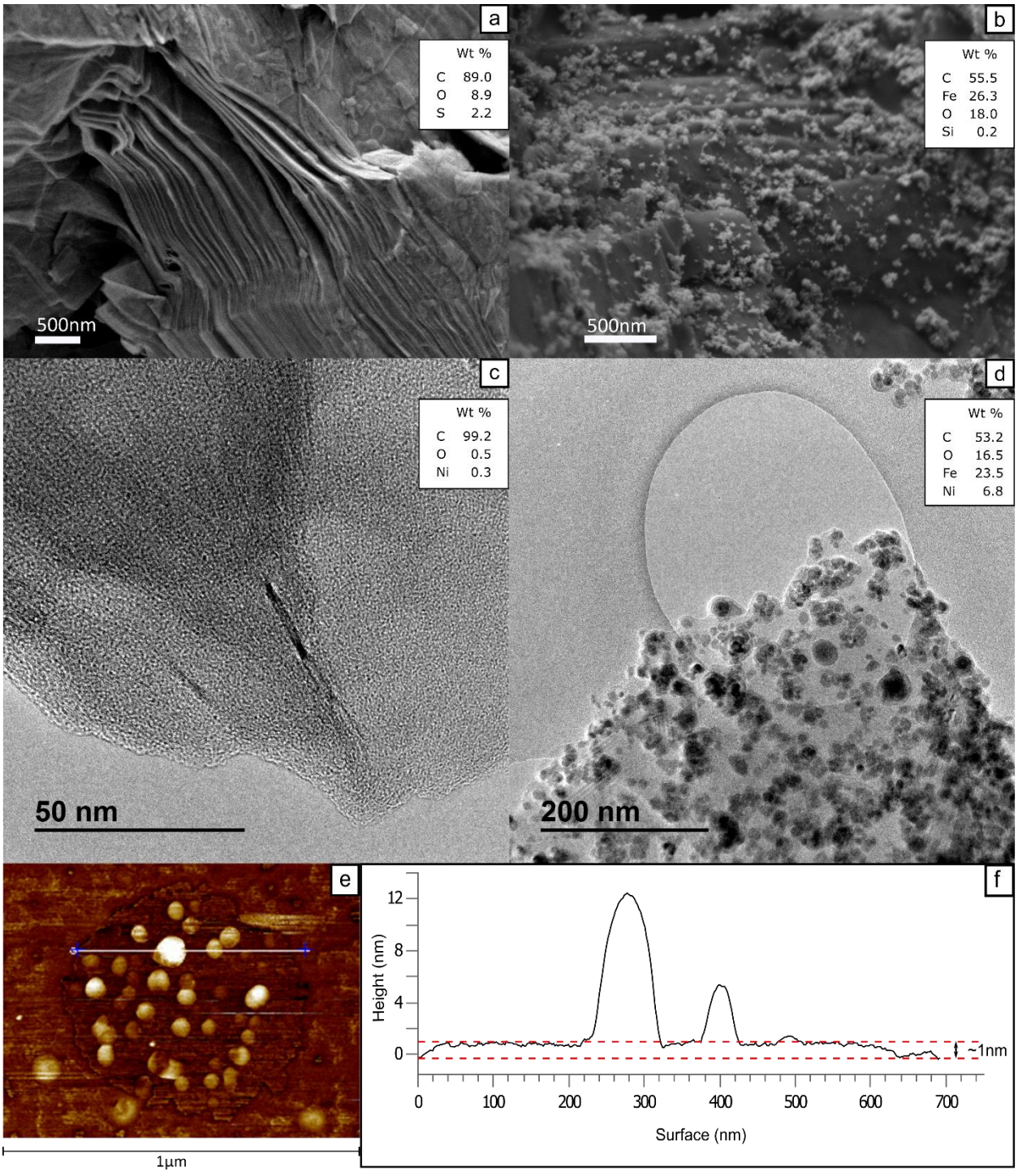

283

284 **Figure 3.** SEM images of **(a)** Graphite oxide and **(b)** Graphite oxide-magnetite. TEM
285 images of **(c)** Graphene oxide and **(d)** Graphene oxide with magnetic nanoparticles
286 (GO-MNP). AFM image of **(e)** Biocatalyst (GO-MNP-Enz) and **(f)** height profile obtained
287 from the indicated line in the AFM image.
288

Evaluation of the immobilization process

The enzyme immobilization process, using different initial protein loads and a constant mass of GO-MNP (mg of protein per g of GO-MNP), was evaluated to determine the yield of protein immobilization (Figure 4a). Higher yields of protein immobilization were observed when low protein loads (up to 50 mg) were applied, which corresponds to approximately 47 mg of protein per g of GO-MNP. When the initial protein load was greater than 50 mg, the yield decreased, but the total amount of protein bound to GO-MNP increased, reaching approximately 140 mg of protein per g of GO-MNP. The amount of protein bounded per g of support using the methodology of EDC-NHS was higher than values reported by previous immobilization studies using other synthetic routes, reaching values between 2.5–52.4 mg of protein per g of support [24,56–58]. Thus, GO-MNP was able to bind a greater amount of protein in its structure when there is an increase in the initial protein load, but excess protein caused a decrease in the yield of protein immobilization. However, despite the fact that the amount of enzyme on GO-MNP increased, the total cellulase activity of the biocatalyst stayed constant at roughly 44 $FPU.g^{-1}$ after an initial protein load of approximately 50 mg per g of GO-MNP. Similar behavior was reported by Alftrén and Hobley [26] using Cellic CTec 2 immobilized in cyanuric chloride-activated magnetic particles, but the activity of its biocatalyst stayed stable at approximately 15.5 $FPU.g^{-1}$ (almost 3x lower than reported herein).

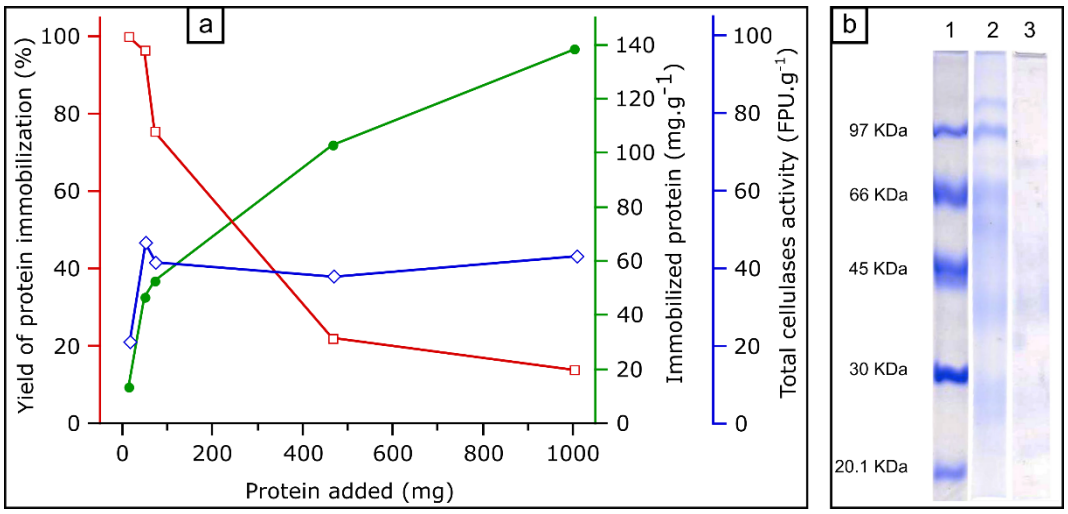

Figure 4. (a) Yield of protein immobilization (%) (□, red), amount of immobilized protein per gram of support (mg.g^{-1}) (●, green) and activity of total cellulases per gram of support (FPU.g^{-1}) (◇, blue) as a function of the protein load of enzymatic preparation Cellic CTec 2. **(b)** Sodium dodecyl sulfate-polyacrylamide gel electrophoresis (SDS-PAGE). Lane 1: molecular weight standards; Lane 2: supernatant before immobilization; Lane 3: supernatant after immobilization.

Sodium dodecyl sulfate-polyacrylamide gel electrophoresis (SDS-PAGE) of the supernatant before and after immobilization is demonstrated in Figure 4b. Using an initial protein load of about 50 mg per g of GO-MNP did not leave meaningful amounts of residual supernatant protein after the immobilization process, confirming the immobilization effectiveness and supporting the protein immobilization yield results.

In summary, starting the immobilization with a protein load of 50 mg of protein per g of GO-MNP led to a yield of 96.5% (Figure 4a). However, because the commercial enzymatic preparation Cellic CTec 2 is a blend of several enzymes (predominantly cellulases and xylanases) and comprises various enzyme activities, it is important to determine the yield of immobilization according to each enzyme activity under the condition of 50 mg of protein per g of GO-MNP. For this purpose, assays for the enzymatic activities of total cellulase, endoglucanase, xylanase, β-glucosidase, and β-

xylosidase were performed in the supernatant (before and after immobilization) and biocatalyst. The assays evaluated the yields of immobilization, efficiency, and activity recovery, ranking between 27%–97%, 37%–113%, and 15%–110%, respectively (Table 1).

Table 1. Yield, efficiency and activity recovery in the immobilization process of enzyme preparation Cellic CTec 2 onto graphene oxide with magnetic nanoparticles (GO-MNP) in the condition with protein load of 50 mg of protein per gram of GO-MNP. Enzymatic activity of the biocatalyst.

Enzyme	Yield of Immobilization (%)	Efficiency (%)	Activity recovery (%)	Biocatalyst activity ($U.g^{-1}$)
Total cellulases	71.1	69.0	49.1	44.1*
Endoglucanase	63.4	37.6	23.8	299.9
Xylanase	27.0	55.2	14.9	1034.0
β-glucosidase	97.2	113.0	109.8	4500.2
β-xylosidase	91.6	86.6	79.3	33.3

* $FPU.g^{-1}$

Xylanase showed the lowest immobilization yield at 27%, indicating that this enzyme is poorly immobilized onto GO-MNP using the method chosen in the present study. However, the enzymatic activity assays showed that the other enzymes were successfully immobilized, presenting immobilization yields of 71%, 63%, 97%, and 92% for total cellulase, endoglucanase, β-glucosidase, and β-xylosidase, respectively.

The efficiency describes the percentage of bound enzyme activity that is verified in the biocatalyst (GO-MNP-Enz) [37]. This value is usually below 100%, likely because of mass transfer limitations, tertiary structure modifications, decreased accessibility of active sites, and solubility of the specific substrate for each enzyme assay. That was the case for all assessed activities except β-glucosidase, which reached 113% efficiency and thus showed improvement in its immobilized form. β-xylosidase also showed a high efficiency (86.6%), indicating that these enzymes are less sensitive to mass transfer issues, presumably because of the high solubility of the specific substrates. β-

glucosidase and β-xylosidase are responsible for the hydrolysis of cellobiose into glucose and xylobiose into xylose, respectively, during the final step of lignocellulose biomass hydrolysis. Therefore, these results are very important for producing a hydrolyzate rich in monomeric sugars.

The activity recovery relates to enzyme activity levels of the biocatalyst (GO-MNP-Enz) compared to the total starting activity of the free enzyme used for immobilization. This number gives an idea of the success of the total immobilization process. The commercial preparation Cellic CTec 2 comprises various enzymatic activities, and the immobilization results of each enzyme were different; β-glucosidase and β-xylosidase presented the best results (110% and 78%, respectively) while xylanase displayed the worst (15%).

The units (μmol.min^{-1}) of enzyme activity per g of biocatalyst were determined (Table 1). The total cellulase activity of the biocatalyst was 44.1 FPU.g^{-1} while the activities of endoglucanase, xylanase, β-glucosidase, and β-xylosidase were 299, 1034, 4500, and 33 U.g^{-1}, respectively. The enzymatic activity assay for exoglucanase was performed using microcrystalline cellulose as the substrate; however, no activity was detected. This could be due to the low activity of the exoglucanase present in commercial enzyme preparation Cellic CTec 2 (0.5 U.mg^{-1} of protein) associated with the dilution that was used for immobilization.

Evaluation of GO-MNP-Enz recyclability

The main objective of the enzyme immobilization was the possibility of reusing the biocatalyst. For this reason, the relative activities of endoglucanase, xylanase, β-

glucosidase, and β-xylosidase after ten hydrolysis cycles of GO-MNP-Enz on their specific substrates were evaluated (Figure 5). GO-MNP-Enz showed relative activities of endoglucanase and xylanase above 85% until the sixth cycle. Furthermore, the endoglucanase activity remained stable at approximately 80% until the ninth cycle and diminished to 70% in the tenth cycle (Figure 5a). The relative enzyme activity of xylanase diminished gradually after the fifth cycle, reaching 66% in the tenth cycle (Figure 5b). The relative activity of β-glucosidase showed an excellent trend, remaining at values above 95% until the ninth cycle and 88% in the last cycle (Figure 5c). The relative activity of β-xylosidase remained stable above 95% until the fifth cycle but then gradually diminished to reach 70% in the tenth cycle (Figure 5d).

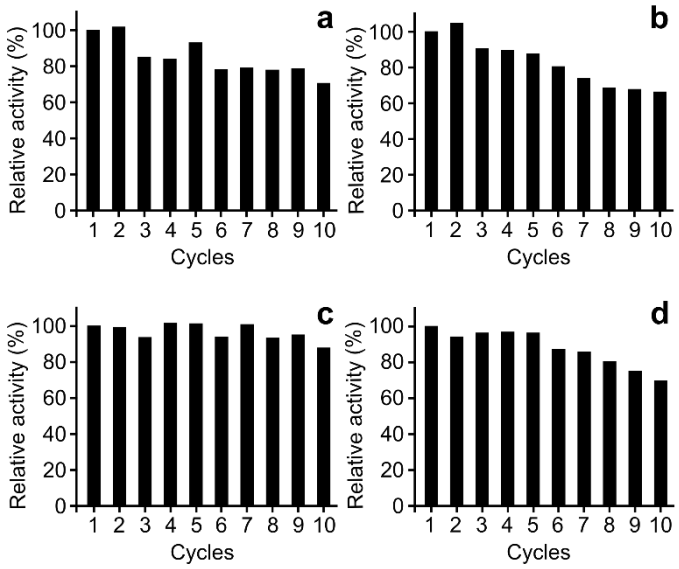

Figure 5. Relative enzyme activity of biocatalyst (GO-MNP-Enz) about their substrates as a function of cycles number of hydrolysis (ten cycles). **(a)** Endoglucanase, **(b)** Xylanase, **(c)** β-glucosidase and **(d)** β-xylosidase.

In order to put the obtained results into perspective, they were confronted with other results recently reported by other authors about the relative activities of endoglucanase, xylanase, β-glucosidase, and β-xylosidase on reuse assays (Table 2).

Several studies have reported about the reuse of β-glucosidase and β-xylosidase immobilized using different strategies and supports [59–68]. A general conclusion obtained by many of those studies is that β-glucosidase can be used for 10 consecutive cycles, conserving between 67%–95% of its initial activity. Also, for β-xylosidase, a relative activity between 39%–95% after 10 cycles of hydrolysis has been identified. These data are in accordance with the findings of this study.

In addition, we can highlight the work by Gao *et al.* [56], who managed to maintain a relative endoglucanase activity of 80% after 9 cycles while Lim *et al.* [69] produced a biocatalyst that maintained a 60% relative xylanase activity after 10 cycles. However, none of the referred systems presented magnetic properties, and deep centrifugation is required before reuse in each experiment. On the other hand, Abraham *et al.*[70] immobilized cellulases on purely magnetite nanoparticles using glutaraldehyde, and the relative activity fell to approximately 30% after 10 cycles of hydrolysis. Gokhale *et al.* [24] and Han *et al.* [71] have used GO-MNP as a support for cellulase immobilization via different routes, but the relative activity of the biocatalyst they obtained fell to approximately 50% after 4 and 7 cycles, respectively. Compared to the results previously reported in the literature for endoglucanase and xylanase reuse, GO-MNP-Enz proved to be stable for more cycles and maintained a greater relative activity.

In addition, the calculated TOF (g of sugar per g of biocatalyst per hour) of the previous reported works are considerably lower than those obtained with our biocatalyst (see Table 2). As can be seen in Table 2, the biocatalyst presented in this work showed a TOF several times higher, reaching 0.40, 2.30, 4.94, and 0.11 h^{-1} using

carboxymethylcellulose (CMC), xylan, 4-Nitrophenyl β-D-glucopyranoside (*p*-NPG), and 4-Nitrophenyl β-D-xylopyranoside (*p*-NPG) as substrates, respectively. These values are especially relevant from the point of view of large-scale production of fermentable sugars.

The main reasons for the superior performance of the biocatalyst presented herein, in comparison to other biocatalysts reported in the literature, are the following: i) the commercial enzyme preparation Cellic CTec 2 is resistant to hydrolysis conditions; ii) the GO kept a high quality (few-layers/high surface area and structural quality) throughout the process; iii) the immobilization method used in combination with the highly hydrophilic characteristics of the high quality GO obtained a consistently supported biocatalyst. Altogether, the resulting GO-MNP-Enz presented not just one but rather all necessary enzymatic activities for lignocellulosic biomass hydrolysis.

Table 2. Literature survey about the relative activity of endocellulase, xylanase β-glucosidase and β-xylosidase after several reuse cycles.

Support	Immobilization route	Number of cycles	Substrate	Relative activity at last cycle (%)	TOF	Reference
MNP	GA	10	CMC	30	0.2586	[70]
GO	SESA	9	CMC	80	0.1193	[56]
MNP	GA	10	CMC	62	0.0026	[57]
GO-MNP	PAA-EDC	4	CMC	55	-	[24]
GO-MNP	PEG10K-GA	7	CMC	45	-	[71]
GO-MNP	EDC-NHS	10	CMC	70	0.4020	This work
Mesoporous cellulose foam	APTES	10	Xylan	60	0.5885	[69]
Zeolite	Adsorption	6	Xylan	56	0.0105	[72]
GO-MNP	PEGA	8	Xylan	10	0.0418	[19]
GO-MNP	EDC-NHS	10	Xylan	66	2.3070	This work
MNP	GA	10	*p*-NPG	86	0.0201	[59]
MNP	APTES-GA	10	*p*-NPG	67	0.3980	[61]
AMNPs	ECH-IDA-Co^{2+}	10	*p*-NPG	95	0.0858	[62]
APEPMOs	Adsorption	10	*p*-NPG	70	-	[63]
GO-MNP	EDC-NHS	10	*p*-NPG	88	4.9450	This work
Chitosan	GA	25	*p*-NPX	94	0.0003	[66]
Agarose	Glyoxyl-PEG	10	*p*-NPX	70	0.0005	[67]
Agarose	Glyoxyl	8	*p*-NPX	40	0.0001	[68]
PAM	Adsorption	10	*p*-NPX	55	-	[65]
GO-MNP	EDC-NHS	10	*p*-NPX	70	0.1133	This work

AMNPs: Agarose coupled to magnetic nanoparticles; APEPMOs: aminopropyl-functionalized ethane-bridged bifunctional periodic mesoporous organosilicas; APTES: (3-Aminopropyl)triethoxysilane; CMC: Sodium carboxymethylcellulose; EDC: 1-ethyl-3-(3-dimethylaminopropyl) carbodiimide; EDH: epichlorohydrin; GA: Glutaraldehyde; GO: Graphene oxide; IDA: iminodiacetatic acid; MCC: Microcrystalline cellulose; MNP: Magnetic nanoparticles; NHS: n-Hydroxysuccinimide; PAA: Polyacrylic acid; PAM: Polyamide membrane; PEG: Polyethylene glycol; PEG10K: 10K-4-arm-PEG-NH_2; PEGA: Poly(ethylene glycol) bis(amine); p-NPG: 4-Nitrophenyl β-D-glucopyranoside; p-NPX: 4-Nitrophenyl β-D-xylopyranoside; SESA: p-β-sulfuric acid ester ethyl sulfone aniline; TOF: Turnover Frequency; WSN: Wrinkled silica nanoparticles; XOs: Xylo-oligosaccharides.

Enzymatic hydrolysis of PSB using GO-MNP-Enz

In order to assess the GO-MNP-Enz performance for a real-life application (compared to its *in vitro* activity), this system was applied to the hydrolysis of PSB, and its conversion was evaluated for 10 reuse cycles (Figure 6). The chemical composition of PSB was determined and reported in Table S1. The enzymatic hydrolysis of PSB reached a 72% conversion of cellulose to glucose in the first cycle. However, the conversion decreased progressively to 56%, 43%, 37%, and 34% in the following four cycles. From the sixth to the ninth cycles, the cellulose conversion to glucose remained stable at approximately 27% (Figure 6).

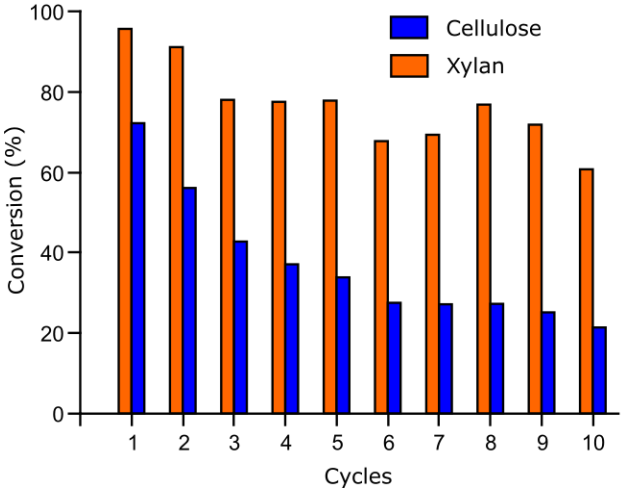

Figure 6. Hydrolysis of sugarcane bagasse pretreated with sulfite-alkali (PSB) with the application of the biocatalyst (GO-MNP-Enz). Cellulose and xylan conversion into glucose and xylose, respectively.

Xylan conversion of PSB to xylose presented more promising results, reaching 96% conversion in the first cycle, 91% in the second cycle, and remaining stable at approximately 78% in the third, fourth, and fifth cycles. From the sixth to the ninth cycles, the conversion remained between 77%–68%, ultimately declining to 61% in the tenth cycle (Figure 6). These results suggested that the biocatalyst presented here kept approximately 50% and 80% of its efficiency for cellulose and xylan hydrolysis, respectively, after 5 hydrolysis cycles. This efficiency was decreased to approximately 65% after 10 cycles of xylan hydrolysis. In general, the loss in efficiency of an enzyme biocatalyst is due to degradation by heat. However, in this work the hydrolysis of sugarcane bagasse was carried out at a moderate temperature (30°C), which probably does not affect the stability of the biocatalyst. A plausible explanation for the loss in efficiency could be small biocatalyst losses in each cycle.

In total, 21 mg of glucose and 20 mg of xylose were produced from 100 mg of PSB after 10 hydrolysis cycles (10 mg of PSB per cycle). Altogether, the biocatalyst presented a satisfactory efficiency, especially for xylan hydrolysis, and is suitable for a cost-effective reuse process.

Previous studies have reported on similar approaches to hydrolyze lignocellulosic biomass; however, some of them applied different pretreatments, such as Ingle *et al.* [73] using cellulase immobilized on MNPs (without GO) for acid PSB and finding a cellulose conversion to glucose of 52%, 47%, and 27% in the first, second, and third cycles, respectively. This means a loss of biocatalyst efficiency of almost 50% by the third cycle. Alftrén and Hobley [26] immobilized the commercial enzymatic preparation Cellic CTec 2 onto MNPs (without GO) activated with cyanuric chloride for hydrolyzing

hydrothermally-pretreated wheat straw (50 °C for 72 h) and identified a cellulose conversion to glucose of 82% in the first hydrolysis cycle and 66% in the second cycle. However, this biocatalyst was only used for two cycles. In another work, cellulases from *Trichoderma reesei* were immobilized in chitosan-coated MNPs and used to hydrolyze *Agave atrovirens* biomass. This biocatalyst was used for 5 hydrolysis cycles, reaching a cellulose conversion to glucose of 22.4% in the first cycle and decreasing to 10.1% in the fifth cycle. This means a loss of biocatalyst efficiency of 55% by the fifth cycle and a production of 6.1 mg of glucose from 100 mg of biomass [74].

The biocatalyst presented in this work reached higher conversion levels and maintained an overall better efficiency. Nonetheless, very few studies have been conducted on biocatalyst reuse in the hydrolysis of real lignocellulosic biomass. Most studies evaluating biocatalyst reuse only utilize model substrates, such as carboxymethyl cellulose (CMC) or microcrystalline cellulose (MCC) [24,56–58,70,71,75–78]. The biocatalyst presented here was capable of being reused for 10 consecutive hydrolysis cycles using real lignocellulosic biomass (PSB). Consequently, GO-MNP-Enz offers an important advantage in the total conversion per biocatalyst life-cycle and could be a prospective candidate for application in industries such as biorefineries.

CONCLUSION

In this study, a commercial enzymatic blend containing cellulases and xylanases was successfully immobilized onto the surface of a GO-magnetite by covalent attachment, producing a biocatalyst (GO-MNP-Enz). The yield, efficiency, and relative

activity of the immobilization process ranked from 27%–97%, 37%–113%, and 24%–110%, respectively, for the different enzymatic activities assessed. This biocatalyst presented a stable behavior when evaluated for the different catalytic activities over several cycles of use, reaching relative endoglucanase, xylanase, β-glucosidase, and β-xylosidase activities of 70%, 66%, 88%, and 70%, respectively, after 10 cycles of hydrolysis. Consequently, the TOF of the GO-MNP-Enz biocatalyst was several times higher than those of other biocatalysts reported in the literature, meaning that more product can be obtained per unit of biocatalyst per h. When GO-MNP-Enz was used multiple times in the hydrolysis of PSB, cellulose conversion to glucose was diminished in comparison to the initial cycles. On the other hand, xylan conversion to xylose, despite decreasing progressively, remained high and stable at levels greater than 60% until the tenth cycle.

Finally, the use of GO-MNP-Enz has been demonstrated as a cost-effective strategy for more competitive hydrolysis of sugarcane bagasse, potentializing its application to the production of second-generation ethanol, where the cost of enzymes is considered the main bottleneck that prevents its economic viability.

DECLARATIONS SECTION

List of abbreviations

(AFM) Atomic force microscopy; (ATR-FTIR) Attenuated total reflection-Fourier Transform Infrared; (CMC) Sodium carboxymethylcellulose; (EDC) 1-ethyl-3-(3-dimethylaminopropyl) carbodiimide; (EDX) Energy-dispersive X-ray; (FPU) Filter paper

units; (GO) Graphene oxide; (GO-MNP) Graphene oxide-magnetite; (GO-MNP-Enz) biocatalyst; (NHS) *N*-hydroxy-succinimide; (PSB) Pretreated sugarcane bagasse; (SEM) Scanning electron microscopy; (SDS-PAGE) sodium dodecyl sulfate–polyacrylamide gel electrophoresis; (TEM) Transmission electron microscopy; (TOF) Turnover frequency.

Ethical Approval and Consent to participate

Not applicable.

Consent for publication

All authors read and approved the final manuscript.

Availability of supporting data

We are providing a document with supplementary information.

Conflicts of interest

There are no conflicts to declare.

Funding

São Paulo State Research Support Foundation (FAPESP) contract number 2018/06241-3 funding this work. Coordination of Improvement of Higher Education Personnel (CAPES) funding the doctoral scholarship of Fernando Roberto Paz-Cedeno in Brazil and in the Universitat Politècnica de València (UPV), Institute of Chemical

Technology (ITQ), Valencia, Spain. Authors acknowledge financial support from PGC2018-097277-B-100(MCIU/AEI/FEDER,UE) project and Severo Ochoa Program (SEV-2016-0683).

CRediT authorship contribution statement

Fernando Roberto Paz Cedeno: Conceptualization, Investigation, Methodology, Writing - original draft, Writing - review & editing. **Jose Miguel Carceller:** Methodology, Writing - review & editing. **Sara Iborra:** Supervision, Funding acquisition, Resources, Writing - review & editing. **Ricardo Keitel Donato:** Supervision, Writing - review & editing. **Anna Paula Godoy:** Methodology, Writing - review & editing. **Ariela Veloso de Paula:** Writing - review & editing. **Rubens Monti:** Writing - review & editing. **Avelino Corma:** Supervision, Funding acquisition, Writing - review & editing. **Fernando Masarin:** Conceptualization, Supervision, Funding acquisition, Resources, Writing - review & editing.

Acknowledgements

FAPESP, contract number 2018/06241-3 funding this paper. Coordination of Improvement of Higher Education Personnel (CAPES) financed the doctoral scholarship of Fernando Roberto Paz-Cedeno in Brazil and in the Universitat Politècnica de València (UPV), Institute of Chemical Technology (ITQ), Valencia, Spain. Authors acknowledge financial support from PGC2018-097277-B-100 (MCIU/AEI/FEDER,UE) project and Program Severo Ochoa (SEV-2016-0683).

REFERENCES

[1] Renewable Fuel Association, 2020 Pocket Guide to Ethanol, 2020. https://ethanolrfa.org/wp-content/uploads/2020/02/2020-Outlook-Pocket-Guide-for-Web.pdf.

[2] UNICA, Moagem de cana-de-açúcar e produção de açúcar e etanol - safra 2018/2019, (2020). http://unicadata.com.br/historico-de-producao-e-moagem.php (accessed February 25, 2020).

[3] V.L. Sirisha, A. Jain, A. Jain, Enzyme Immobilization: An Overview on Methods, Support Material, and Applications of Immobilized Enzymes, Adv. Food Nutr. Res. 79 (2016) 179–211. doi:10.1016/bs.afnr.2016.07.004.

[4] C. Aragon, Imobilização multipontual covalente de xilanases: seleção de derivados ativos e estabilizados, Universidade Estadual Paulista Julio de Mesquita Filho, 2013.

[5] S. Lei, Y. Xu, G. Fan, M. Xiao, S. Pan, Immobilization of naringinase on mesoporous molecular sieve MCM-41 and its application to debittering of white grapefruit, Appl. Surf. Sci. 257 (2011) 4096–4099. doi:10.1016/j.apsusc.2010.12.003.

[6] J.M. Guisán, Immobilization of enzymes on glyoxyl agarose – Strategies for enzyme stabilization by multipoint attachment, in: G.F. BICKERSTAFF (Ed.), Immobil. Enzym. Cells, 1st ed., Humana Press, Totowa, 1997: pp. 277–287. doi:10.1385/0896033864.

[7] J.M. Guisan, Aldehyde-agarose gels as activated supports for immobilization-stabilization of enzymes, Enzyme Microb. Technol. 10 (1988) 375–382.

592 doi:10.1016/0141-0229(88)90018-X.
593 [8] J. Jiang, J. Zhao, C. He, B. Cui, J. Xiong, H. Jiang, J. Ao, G. Xiang, Recyclable
594 magnetic carboxymethyl chitosan/calcium alginate – cellulase bioconjugates for
595 corn stalk hydrolysis, Carbohydr. Polym. 166 (2017) 358–364.
596 doi:10.1016/j.carbpol.2017.03.003.
597 [9] E. Poorakbar, A. Shafiee, A.A. Saboury, B.L. Rad, K. Khoshnevisan, L. Ma'mani,
598 H. Derakhshankhah, M.R. Ganjali, M. Hosseini, Synthesis of magnetic gold
599 mesoporous silica nanoparticles core shell for cellulase enzyme immobilization:
600 Improvement of enzymatic activity and thermal stability, Process Biochem. 71
601 (2018) 92–100. doi:10.1016/j.procbio.2018.05.012.
602 [10] N.R. Mohamad, N. Haziqah, C. Marzuki, N.A. Buang, R.A. Wahab, An overview of
603 technologies for immobilization of enzymes and surface analysis techniques for
604 immobilized enzymes, Biotechnol. Biotechnol. Equip. 29 (2015) 205–220.
605 doi:10.1080/13102818.2015.1008192.
606 [11] I. Díaz Carretero, R.M. Blanco Martín, M. Sánchez Sánchez, C. Márquez Álvarez,
607 Biocatalysis on porous materials, in: V. Blay, L.F. Bobadilla, A. Cabrera-García
608 (Eds.), Zeolites Met. Fram. From Lab to Ind., Amsterdam University Press, 2018:
609 pp. 149–174. http://hdl.handle.net/10261/164226.
610 [12] J.M. Carceller, R. Monti, J.C. Bassan, M. Filice, J. Yu, S. Iborra, Covalent
611 immobilization of naringinase over two-dimensional 2D zeolites and its
612 applications in a continuous process to produce citrus flavonoids and for
613 debittering of juices, ChemCatChem. (2020). doi:10.1002/cctc.202000320.
614 [13] P. Miró, M. Audiffred, T. Heine, An atlas of two-dimensional materials, Chem.

Soc. Rev. 43 (2014) 6537–6554. doi:10.1039/c4cs00102h.

[14] P. Montes-Navajas, N.G. Asenjo, R. Santamaría, R. Menéndez, A. Corma, H. García, Surface Area Measurement of Graphene Oxide in Aqueous Solutions, Langmuir. 29 (2013) 13443–13448. doi:10.1021/la4029904.

[15] J. Zhang, J. Zhang, F. Zhang, H. Yang, X. Huang, H. Liu, S. Guo, Graphene oxide as a matrix for enzyme immobilization, Langmuir. 26 (2010) 6083–6085. doi:10.1021/la904014z.

[16] J.M. Carceller, J.P. Martínez Galán, R. Monti, J.C. Bassan, M. Filice, S. Iborra, J. Yu, A. Corma, Selective synthesis of citrus flavonoids prunin and naringenin using heterogeneized biocatalyst on graphene oxide, Green Chem. 21 (2019) 839–849. doi:10.1039/c8gc03661f.

[17] E. Doustkhah, S. Rostamnia, Covalently bonded sulfonic acid magnetic graphene oxide: Fe3O4@GO-Pr-SO3H as a powerful hybrid catalyst for synthesis of indazolophthalazinetriones, J. Colloid Interface Sci. 478 (2016) 280–287. doi:10.1016/j.jcis.2016.06.020.

[18] M. Heidarizadeh, E. Doustkhah, S. Rostamnia, P.F. Rezaei, F.D. Harzevili, B. Zeynizadeh, Dithiocarbamate to modify magnetic graphene oxide nanocomposite (Fe3O4-GO): A new strategy for covalent enzyme (lipase) immobilization to fabrication a new nanobiocatalyst for enzymatic hydrolysis of PNPD, Int. J. Biol. Macromol. 101 (2017) 696–702. doi:10.1016/j.ijbiomac.2017.03.152.

[19] V. Mehnati-Najafabadi, A. Taheri-Kafrani, A.K. Bordbar, Xylanase immobilization on modified superparamagnetic graphene oxide nanocomposite: Effect of PEGylation on activity and stability, Int. J. Biol. Macromol. 107 (2018) 418–425.

638 doi:10.1016/j.ijbiomac.2017.09.013.
639 [20] C.G.C.M. Netto, H.E. Toma, L.H. Andrade, Superparamagnetic nanoparticles as
640 versatile carriers and supporting materials for enzymes, J. Mol. Catal. B Enzym.
641 85–86 (2013) 71–92. doi:10.1016/j.molcatb.2012.08.010.
642 [21] W. Huang, S. Pan, Y. Li, L. Yu, R. Liu, Immobilization and Characterization of
643 cellulase on hydroxy and aldehyde functionalized magnetic Fe2O3/Fe3O4
644 nanocomposites prepared via a novel rapid combustion process, Int. J. Biol.
645 Macromol. 162 (2020) 845–852.
646 doi:https://doi.org/10.1016/j.ijbiomac.2020.06.209.
647 [22] R. Liu, W. Huang, S. Pan, Y. Li, L. Yu, D. He, Covalent immobilization and
648 characterization of penicillin G acylase on magnetic Fe2O3/Fe3O4
649 heterostructure nanoparticles prepared via a novel solution combustion and gel
650 calcination process, Int. J. Biol. Macromol. 162 (2020) 1587–1596.
651 doi:10.1016/j.ijbiomac.2020.07.283.
652 [23] K. Khoshnevisan, F. Vakhshiteh, M. Barkhi, H. Baharifar, E. Poor-Akbar, N. Zari,
653 H. Stamatis, A.K. Bordbar, Immobilization of cellulase enzyme onto magnetic
654 nanoparticles: Applications and recent advances, Mol. Catal. 442 (2017) 66–73.
655 doi:10.1016/j.mcat.2017.09.006.
656 [24] A.A. Gokhale, J. Lu, I. Lee, Immobilization of cellulase on magnetoresponsive
657 graphene nano-supports, J. Mol. Catal. B Enzym. 90 (2013) 76–86.
658 doi:10.1016/j.molcatb.2013.01.025.
659 [25] Y. Lin, X. Liu, Z. Xing, Y. Geng, J. Wilson, D. Wu, H. Kong, Preparation and
660 characterization of magnetic Fe3O4–chitosan nanoparticles for cellulase

661 immobilization, Cellulose. 24 (2017) 5541–5550. doi:10.1007/s10570-017-1520-6.
662 [26] J. Alftrén, T.J. Hobley, Immobilization of cellulase mixtures on magnetic particles
663 for hydrolysis of lignocellulose and ease of recycling, Biomass and Bioenergy. 65
664 (2014) 72–78. doi:10.1016/j.biombioe.2014.03.009.
665 [27] R. Ahmad, M. Sardar, Immobilization of cellulase on TiO2 nanoparticles by
666 physical and covalent methods: A comparative study, Indian J. Biochem. Biophys.
667 51 (2014) 314–320.
668 [28] H. Liao, D. Chen, L. Yuan, M. Zheng, Y. Zhu, X. Liu, Immobilized cellulase by
669 polyvinyl alcohol/Fe2O3magnetic nanoparticle to degrade microcrystalline
670 cellulose, Carbohydr. Polym. 82 (2010) 600–604.
671 doi:10.1016/j.carbpol.2010.05.021.
672 [29] M. Sakata, A. Funatsu, S. Sonoda, T. Ogata, T. Taniguchi, Y. Matsumoto,
673 Immobilization of Trypsin on Graphene Oxide Nanosheets for Increased
674 Proteolytic Stability, Chem. Lett. 41 (2012) 1625–1627. doi:10.1246/cl.2012.1625.
675 [30] J. Shen, M. Shi, B. Yan, H. Ma, N. Li, Y. Hu, M. Ye, Covalent attaching protein to
676 graphene oxide via diimide-activated amidation, Colloids Surfaces B
677 Biointerfaces. 81 (2010) 434–438. doi:10.1016/j.colsurfb.2010.07.035.
678 [31] Q. Yu, Z. Wang, Y. Zhang, R. Liu, Covalent immobilization and characterization of
679 penicillin G acylase on amino and GO functionalized magnetic
680 Ni0.5Zn0.5Fe2O4@SiO2 nanocomposite prepared via a novel rapid-combustion
681 process, Int. J. Biol. Macromol. 134 (2019) 507–515.
682 doi:10.1016/j.ijbiomac.2019.05.066.
683 [32] W.S. Hummers, R.E. Offeman, Preparation of Graphitic Oxide, J. Am. Chem. Soc.

684 80 (1958) 1339–1339. doi:10.1021/ja01539a017.
685 [33] T.K. Ghose, Measurement of cellulase activities, Pure Appl. Chem. 59 (1987)
686 257–268. doi:10.1351/pac198759020257.
687 [34] M. Tanaka, M. Taniguchi, R. Matsuno, T. Kamikubo, Purification and Properties of
688 Cellulases from Eupencillium javanicum : Studies on the Re-utilization of
689 Cellulosic Resources(VII), J. Ferment. Technol. 59 (1981) 177–183.
690 http://ci.nii.ac.jp/naid/110002672575/en/ (accessed July 26, 2016).
691 [35] M.J. Bailey, P. Biely, K. Poutanen, Interlaboratory testing of methods for assay of
692 xylanase activity, J. Biotechnol. 23 (1992) 257–270. doi:10.1016/0168-
693 1656(92)90074-J.
694 [36] L.U.L. Tan, P. Mayers, J.N. Saddler, Purification and characterization of a
695 thermostable xylanase from a thermophilic fungus Thermoascus aurantiacus,
696 Can. J. Microbiol. (1987) 689–691. doi:10.1139/m87-120.
697 [37] R.A. Sheldon, S. van Pelt, Enzyme immobilisation in biocatalysis: Why, what and
698 how, Chem. Soc. Rev. 42 (2013) 6223–6235. doi:10.1039/c3cs60075k.
699 [38] F.M. Mendes, G. Siqueira, W. Carvalho, A. Ferraz, A.M.F. Milagres, Enzymatic
700 hydrolysis of chemithermomechanically pretreated sugarcane bagasse and
701 samples with reduced initial lignin content, Biotechnol. Prog. 27 (2011) 395–401.
702 doi:10.1002/btpr.553.
703 [39] F.R. Paz-Cedeno, E.G. Solórzano-Chávez, L.E. de Oliveira, V.C. Gelli, R. Monti,
704 S.C. de Oliveira, F. Masarin, Sequential Enzymatic and Mild-Acid Hydrolysis of
705 By-Product of Carrageenan Process from Kappaphycus alvarezii, BioEnergy Res.
706 12 (2019) 419–432. doi:10.1007/s12155-019-09968-7.

[40] E.G. Solorzano-Chavez, F.R. Paz-Cedeno, L. Ezequiel de Oliveira, V.C. Gelli, R. Monti, S. Conceição de Oliveira, F. Masarin, Evaluation of the Kappaphycus alvarezii growth under different environmental conditions and efficiency of the enzymatic hydrolysis of the residue generated in the carrageenan processing, Biomass and Bioenergy. 127 (2019). doi:10.1016/j.biombioe.2019.105254.

[41] F. Masarin, F.R.P. Cedeno, E.G.S. Chavez, L.E. de Oliveira, V.C. Gelli, R. Monti, Chemical analysis and biorefinery of red algae Kappaphycus alvarezii for efficient production of glucose from residue of carrageenan extraction process, Biotechnol. Biofuels. 9 (2016) 122. doi:10.1186/s13068-016-0535-9.

[42] Q. Zhang, J. Kang, B. Yang, L. Zhao, Z. Hou, B. Tang, Immobilized cellulase on Fe3O4nanoparticles as a magnetically recoverable biocatalyst for the decomposition of corncob, Cuihua Xuebao/Chinese J. Catal. 37 (2016) 389–397. doi:10.1016/S1872-2067(15)61028-2.

[43] P.J. Huang, K.L. Chang, J.F. Hsieh, S.T. Chen, Catalysis of rice straw hydrolysis by the combination of immobilized cellulase from aspergillus niger on β - Cyclodextrin-Fenanoparticles and ionic liquid, Biomed Res. Int. 2015 (2015). doi:10.1155/2015/409103.

[44] X. Yang, X. Zhang, Y. Ma, Y. Huang, Y. Wang, Y. Chen, Superparamagnetic graphene oxide-Fe3O4 nanoparticles hybrid for controlled targeted drug carriers, J. Mater. Chem. 19 (2009) 2710–2714. doi:10.1039/b821416f.

[45] M.I. Khalil, Co-precipitation in aqueous solution synthesis of magnetite nanoparticles using iron(III) salts as precursors, Arab. J. Chem. 8 (2015) 279–284. doi:10.1016/j.arabjc.2015.02.008.

730 [46] U. Han, M. Choi, J. Hong, Immobilization of basic fibroblast growth factor on
731 heparin/EDC-methiodide nano-aggregates to maintain its continuous signaling, J.
732 Ind. Eng. Chem. 53 (2017) 404–410. doi:10.1016/j.jiec.2017.05.012.
733 [47] M. Bagherzadeh, M.A. Amrollahi, S. Makizadeh, Decoration of Fe3O4magnetic
734 nanoparticles on graphene oxide nanosheets, RSC Adv. 5 (2015) 105499–
735 105506. doi:10.1039/c5ra22315f.
736 [48] M. Puche Panadero, Nanomateriales híbridos basados en complejos de metales
737 de transición anclados sobre óxido de grafeno. Aplicaciones catalíticas.,
738 Universitat Politècnica de València, 2017. doi:10.4995/Thesis/10251/86211.
739 [49] M.A. Pimenta, G. Dresselhaus, M.S. Dresselhaus, L.G. Cançado, A. Jorio, R.
740 Saito, Studying disorder in graphite-based systems by Raman spectroscopy,
741 Phys. Chem. Chem. Phys. 9 (2007) 1276–1290. doi:10.1039/B613962K.
742 [50] D.C. Elias, R.R. Nair, T.M.G. Mohiuddin, S. V Morozov, P. Blake, M.P. Halsall,
743 A.C. Ferrari, D.W. Boukhvalov, M.I. Katsnelson, A.K. Geim, K.S. Novoselov,
744 Control of Graphene Properties by Reversible Hydrogenation: Evidence for
745 Graphane, Science (80-.). 323 (2009) 610 LP – 613.
746 doi:10.1126/science.1167130.
747 [51] C. Xu, X. Wang, J. Zhu, Graphene−Metal Particle Nanocomposites, J. Phys.
748 Chem. C. 112 (2008) 19841–19845. doi:10.1021/jp807989b.
749 [52] T. Szabó, E. Tombácz, E. Illés, I. Dékány, Enhanced acidity and pH-dependent
750 surface charge characterization of successively oxidized graphite oxides, Carbon
751 N. Y. 44 (2006) 537–545. doi:10.1016/j.carbon.2005.08.005.
752 [53] S. Zhang, H. Wang, J. Liu, C. Bao, Measuring the specific surface area of

753 monolayer graphene oxide in water, Mater. Lett. 261 (2020) 127098.
754 doi:10.1016/j.matlet.2019.127098.
755 [54] S. Yusan, Preparation and characterization of magnetic graphene oxide
756 nanocomposite (GO-Fe3O4) for removal of strontium and cesium from aqueous
757 solutions, Compos. Mater. Res. 7 (2018). doi:10.18282/cmr.v7i1.89.
758 [55] P. Wang, X. Zhou, Y. Zhang, L. Wang, K. Zhi, Y. Jiang, Synthesis and application
759 of magnetic reduced graphene oxide composites for the removal of bisphenol A in
760 aqueous solution—a mechanistic study, RSC Adv. 6 (2016) 102348–102358.
761 doi:10.1039/C6RA23542E.
762 [56] J. Gao, C.-L. Lu, Y. Wang, S.-S. Wang, J.-J. Shen, J.-X. Zhang, Y.-W. Zhang,
763 Rapid immobilization of cellulase onto graphene oxide with a hydrophobic spacer,
764 Catalysts. 8 (2018) 1–12. doi:10.3390/catal8050180.
765 [57] K. Selvam, M. Govarthanan, D. Senbagam, S. Kamala-Kannan, B. Senthilkumar,
766 T. Selvankumar, Activity and stability of bacterial cellulase immobilized on
767 magnetic nanoparticles, Cuihua Xuebao/Chinese J. Catal. 37 (2016) 1891–1898.
768 doi:10.1016/S1872-2067(16)62487-7.
769 [58] J. Jordan, C.S.S.R. Kumar, C. Theegala, Preparation and characterization of
770 cellulase-bound magnetite nanoparticles, J. Mol. Catal. B Enzym. 68 (2011) 139–
771 146. doi:10.1016/j.molcatb.2010.09.010.
772 [59] Y. Zhou, S. Pan, X. Wei, L. Wang, Y. Liu, Immobilization of β-glucosidase onto
773 magnetic nanoparticles and evaluation of the enzymatic properties,
774 BioResources. 8 (2013) 2605–2619. doi:10.15376/biores.8.2.2605-2619.
775 [60] V. Califano, F. Sannino, A. Costantini, J. Avossa, S. Cimino, A. Aronne, Wrinkled

776 Silica Nanoparticles: Efficient Matrix for β-Glucosidase Immobilization, J. Phys.
777 Chem. C. 122 (2018) 8373–8379. doi:10.1021/acs.jpcc.8b00652.
778 [61] H.J. Park, A.J. Driscoll, P.A. Johnson, The development and evaluation of B-
779 glucosidase immobilized magnetic nanoparticles as recoverable biocatalysts,
780 Biochem. Eng. J. 133 (2018) 66–73. doi:10.1016/j.bej.2018.01.017.
781 [62] T. Chen, W. Yang, Y. Guo, R. Yuan, L. Xu, Y. Yan, Enhancing catalytic
782 performance of β-glucosidase via immobilization on metal ions chelated magnetic
783 nanoparticles, Enzyme Microb. Technol. 63 (2014) 50–57.
784 doi:10.1016/j.enzmictec.2014.05.008.
785 [63] L. Guan, B. Di, M. Su, J. Qian, Immobilization of β-glucosidase on bifunctional
786 periodic mesoporous organosilicas, Biotechnol. Lett. 35 (2013) 1323–1330.
787 doi:10.1007/s10529-013-1208-4.
788 [64] A. Morana, A. Mangione, L. Maurelli, I. Fiume, O. Paris, R. Cannio, M. Rossi,
789 Immobilization and characterization of a thermostable β-xylosidase to generate a
790 reusable biocatalyst, Enzyme Microb. Technol. 39 (2006) 1205–1213.
791 doi:10.1016/j.enzmictec.2006.03.010.
792 [65] G. Delcheva, G. Dobrev, I. Pishtiyski, Performance of Aspergillus niger B 03 β-
793 xylosidase immobilized on polyamide membrane support, J. Mol. Catal. B Enzym.
794 54 (2008) 109–115. doi:10.1016/j.molcatb.2007.12.019.
795 [66] M. Guerfali, I. Maalej, A. Gargouri, H. Belghith, Catalytic properties of the
796 immobilized Talaromyces thermophilus β-xylosidase and its use for xylose and
797 xylooligosaccharides production, J. Mol. Catal. B Enzym. 57 (2009) 242–249.
798 doi:10.1016/j.molcatb.2008.09.011.

[67] C.R.F. Terrasan, M. Romero-Fernández, A.H. Orrego, S.M. Oliveira, B.C. Pessela, E.C. Carmona, J.M. Guisan, Immobilization and Stabilization of Beta-Xylosidases from Penicillium janczewskii, Appl. Biochem. Biotechnol. 182 (2017) 349–366. doi:10.1007/s12010-016-2331-1.

[68] C.R.F. Terrasan, C.C. Aragon, D.C. Masui, B.C. Pessela, G. Fernandez-Lorente, E.C. Carmona, J.M. Guisan, β-xylosidase from Selenomonas ruminantium: Immobilization, stabilization, and application for xylooligosaccharide hydrolysis, Biocatal. Biotransformation. 34 (2016) 161–171. doi:10.1080/10242422.2016.1247817.

[69] H.K. Lim, N.-J. Park, Y.K. Hwang, K.-I. Lee, T. Hwang, Improvement and Immobilization of a new Endo-β-1,4-xylanases KRICT PX1 from Paenibacillus sp. HPL-001, J. Bioprocess. Biotech. 05 (2015) 1–8. doi:10.4172/2155-9821.1000215.

[70] R.E. Abraham, M.L. Verma, C.J. Barrow, M. Puri, Suitability of magnetic nanoparticle immobilised cellulases in enhancing enzymatic saccharification of pretreated hemp biomass, Biotechnol. Biofuels. 7 (2014) 1–12. doi:10.1186/1754-6834-7-90.

[71] J. Han, P. Luo, Y. Wang, L. Wang, C. Li, W. Zhang, J. Dong, L. Ni, The development of nanobiocatalysis via the immobilization of cellulase on composite magnetic nanomaterial for enhanced loading capacity and catalytic activity, Int. J. Biol. Macromol. 119 (2018) 692–700. doi:10.1016/j.ijbiomac.2018.07.176.

[72] J. Na'imah, S. Prasetyawan, A. Srihardyastutie, In Vitro and In Silico Studies of Immobilized Xylanase on Zeolite Matrix Activated with Hydrochloric Acid, J. Pure

Appl. Chem. Res. 6 (2017) 181–188. doi:10.21776/ub.jpacr.2017.006.03.335.

[73] A.P. Ingle, J. Rathod, R. Pandit, S.S. da Silva, M. Rai, Comparative evaluation of free and immobilized cellulase for enzymatic hydrolysis of lignocellulosic biomass for sustainable bioethanol production, Cellulose. 24 (2017) 5529–5540. doi:10.1007/s10570-017-1517-1.

[74] J. Sánchez-Ramírez, J.L. Martínez-Hernández, P. Segura-Ceniceros, G. López, H. Saade, M.A. Medina-Morales, R. Ramos-González, C.N. Aguilar, A. Ilyina, Cellulases immobilization on chitosan-coated magnetic nanoparticles: application for Agave Atrovirens lignocellulosic biomass hydrolysis, Bioprocess Biosyst. Eng. 40 (2017) 9–22. doi:10.1007/s00449-016-1670-1.

[75] J. Han, L. Wang, Y. Wang, J. Dong, X. Tang, L. Ni, L. Wang, Preparation and characterization of Fe3O4-NH2@4-arm-PEG-NH2, a novel magnetic four-arm polymer-nanoparticle composite for cellulase immobilization, Biochem. Eng. J. 130 (2018) 90–98. doi:10.1016/j.bej.2017.11.008.

[76] T. Alahakoon, J.W. Koh, X.W.C. Chong, W.T.L. Lim, Immobilization of cellulases on amine and aldehyde functionalized Fe2O3magnetic nanoparticles, Prep. Biochem. Biotechnol. 42 (2012) 234–248. doi:10.1080/10826068.2011.602800.

[77] J. Xu, Z. Sheng, X. Wang, X. Liu, J. Xia, P. Xiong, B. He, Enhancement in ionic liquid tolerance of cellulase immobilized on PEGylated graphene oxide nanosheets: Application in saccharification of lignocellulose, Bioresour. Technol. 200 (2016) 1060–1064. doi:10.1016/j.biortech.2015.10.070.

[78] M.R. Ladole, J.S. Mevada, A.B. Pandit, Ultrasonic hyperactivation of cellulase immobilized on magnetic nanoparticles, Bioresour. Technol. 239 (2017) 117–126.

845 doi:10.1016/j.biortech.2017.04.096.

846